IEEE POWER & ENERGY SOCIETY SECTION

IEEE Access
Multidisciplinary : Rapid Review : Open Access Journal

Received January 8, 2021, accepted February 14, 2021, date of publication February 18, 2021, date of current version March 1, 2021.

Digital Object Identifier 10.1109/ACCESS.2021.3060018

Efficiency Optimization of IPOP DC/DC System for HEV

FENGWANG LU, LIANGZONG HE, QINGYANG TAN, AND HONGYAN ZHOU
School of Aeronautics and Astronautics, Xiamen University, Xiamen 361000, China

Corresponding author: Liangzong He (hlz190213@163.com)

This work was supported in part by the National Nature Science Foundation of China under Grant 62071406, and in part by the Fujian Province Outstanding Youth Fund under Grant 2018J06016.

ABSTRACT Input parallel output parallel (IPOP) DC/DC system is widely utilized in many occasions like data center and hybrid electric vehicle (HEV). However, the efficiency characteristics of different converters usually differs from each other, and the conventional control strategy has difficult to realize efficient conversion of overall power of the system. To address this issue, Buck converter is taken as the module and whose efficiency model under current continuous conduction mode (CCM) is presented. Meantime, parameter identification method based on least square (LS) algorithm is proposed as well. In order to realize the efficiency optimization of the whole parallel system, the constraint conditions of each module are analyzed, and the current distribution calculation method based on sequential quadratic programming (SQP) algorithm for the parallel system is introduced. On this basis, a control strategy of proportional current distribution (PCD) is proposed, which not only ensures that the parallel system can always run as efficiently as possible under different loads, but also realizes the flexible switching between the current-sharing mode and current distribution mode. Finally, the simulation and experimental results prove that the proposed method can achieve 4.46% higher efficiency than conventional method within the given power range of each converter, and realize the efficiency optimization of the IPOP DC/DC system to the greatest extent.

INDEX TERMS Efficiency optimization, LS algorithm, proportional current distribution, IPOP DC/DC converter, SQP algorithm.

I. INTRODUCTION

A. BACKGROUND

In response to the call of energy conservation and emission reduction, countries around the world are vigorously developing the new energy vehicle industry, and it is expected that the sales volume will continue to grow substantially in 2020 [1], [2]. Meanwhile, with the increasing power of on-board electrical appliances, the design of conventional DC/DC power supply system is also presented a great challenge. Therefore, multiple small and medium power DC/DC converters are combined into a high-power IPOP DC/DC system by means of input parallel output parallel (IPOP), which is an excellent power supply scheme for hybrid electric vehicle. The power distribution of HEV is shown in Fig.1. On the one hand, the parallel connection of the converter can facilitate the power expansion, alleviate the current stress of the semiconductor device, and extend the service life. On the other hand, it can also leave a huge space for the system efficiency optimization due to the differences for each converter.

For the IPOP DC/DC system, the research mainly focuses on the coordination control and efficiency optimization between converters, which are reported in [3]–[10]. Moreover, the study of step-down DC/DC topology is also an important direction, and a lot of work has been done in [11]–[14]. At present, current-sharing control methods are mostly adopted in the IPOP DC/DC system. Furthermore, by dynamic phase add/drop mechanism, an interesting optimization approach are presented in [15]–[17], in which the efficiency characteristic relationship among different modes is discussed. However, the research fails to consider the efficiency optimization of the IPOP DC/DC system with an optimal number of converters working. Due to the existence of parasitic parameters, the efficiency characteristics of each module are different. Usually, the converter only reaches its efficiency peak at a certain output power point and the efficiency will decrease when it goes far away from that point. Therefore, it is a challenge to have all the modular converters work in their optimum efficiency point.

The associate editor coordinating the review of this manuscript and approving it for publication was Guangya Yang.

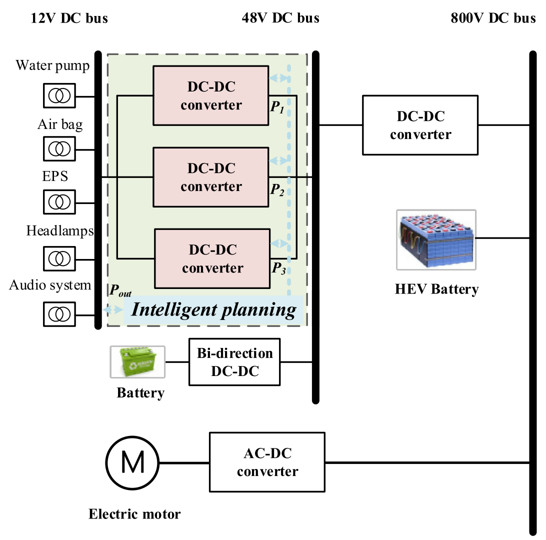

FIGURE 1. The power distribution of HEV.

B. SYSTEM EFFICIENCY OPTIMIZATION CONSIDERATION

Aiming at the efficient DC/DC system, most work realizes the efficiency optimization based on the loss analysis of converter self. Literature [18] analyzes the loss and power density of the DC/DC converter, establishes the corresponding mathematical model, and realizes the multi-objective optimization of DC/DC converter using geometric programming. Although it provides an excellent way to achieve global optimal efficiency of the DC/DC system, the theoretical analysis has complicated procedure and poor generality. Lagrange multiplier method is reported in [19], [20], in which the optimal current distribution solutions of each converter is derived by the loss model of the converter, and the efficiency optimization of the system is realized. Nevertheless, considering the power limitation of the converter, the IPOP system efficiency becomes an optimization problem with multivariate equality and inequality constraints. The issue with multivariate inequality constraint cannot be calculated out by means of the Lagrange multiplier method, so the scheme proposed in the above literatures also have quadratic optimization regulation, which makes the problem more complex. Advanced algorithms such as genetic algorithm, particle swarm optimization and game theory are presented in [21]–[23] to verify the feasibility of achieving efficiency optimization. However, these advanced algorithms are prone to fall into local optimal solutions, and there is no effective quantitative analysis method for the feasibility, accuracy and complexity of the algorithm, which cannot guarantee the effect of efficiency optimization.

To address above issue, in this paper, the LS algorithm is employed to identify the efficiency model of each converter. On this basis, the current distribution coefficient matrix $\boldsymbol{K}$ of each converter at the optimal efficiency of the system is obtained by SQP algorithm. The SQP algorithm is used to adjust the current distribution coefficient matrix $\boldsymbol{K}$ when the load changes, so as to ensure efficient operation of the

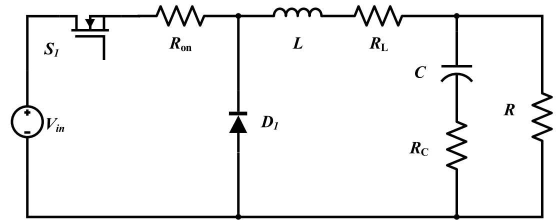

FIGURE 2. Buck converter topology.

IPOP DC/DC system and avoid secondary optimization regulation. Furthermore, a control strategy based on proportional current distribution is proposed. The proposed strategy can also realize the flexible switching of the current-sharing and current distribution mode, which is convenient for the design of over current protection.

The paper is organized as follow: the proposed optimization strategy is introduced, and the mathematical model of IPOP DC/DC system is analyzed in Section II. The proposed control strategy and framework is described in Section III. Sequentially, the simulation and experimental results are analyzed in Section IV. Then, the conclusion is presented in Section V.

II. EFFICIENCY ANALYSIS OF IPOP DC/DC SYSTEM

As shown in Fig.1, after the step-down conversion from the high-voltage bus (the motor inverter output), part of the energy is stored in the battery by bi-direction DC/DC converter. It is also discharged when the car is idle and charged when the car is braking. In addition, the on-board electrical appliances can be briefly powered by the 48V battery when the vehicle is stationary. Most of the energy is transferred to the vehicle electrical appliances through the proposed IPOP DC/DC converter system, which is shown in the dark section. The rated power of the converter is extended by the IPOP structure. Since the voltage of the high/low voltage bus is constant, the power distribution between modules can be equivalent to the current distribution. By establishing the efficiency model of the converter, where the corresponding constraints are taken into consideration, the power distribution under the global optimal efficiency condition can be deduced. Finally, the system can be controlled in real-time according to the load demand, to ensure the global optimal efficiency.

In this paper, a typical DC/DC Buck converter is taken as the module unit in the IPOP system, as shown in Fig.2. The losses are mainly concentrated on the semiconductor devices caused by switch and conduction of semiconductor devices. Moreover, the parasitic resistance of inductance and capacitance also consumes part of energy. The total loss nonlinearly changes with the variation of current. Generally, the efficiency reaches the optimal level at 30%-60% of the rated load current.

A. THE EFFICIENCY MODEL OF DC/DC CONVERTER

Unlike conventional polynomial function fitting, the derivative of the exponential function (1) has at most one zero point, which has little influence on over-fitting and is consistent

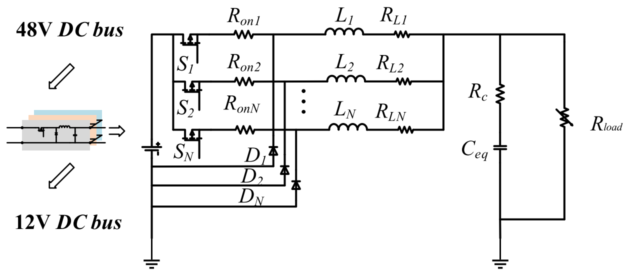

FIGURE 3. The equivalent circuit of DC/DC system framework.

with the typical efficiency characteristic curve. Therefore, the exponential function (1) is chosen as the efficiency model of the Buck converter.

$$\eta_{\mathrm{i}} = ae^{bI_{\mathrm{o}}} + ce^{dI_{\mathrm{o}}} \tag{1}$$

where, the output current of each module is I_{io} (i = 1, 2, ..., n), and a, b, c, d are specific parameters.

Due to the difference in modules parasitic parameters, it is impossible to ensure that all modules operate at the optimal efficiency for the IPOP DC/DC system. Therefore, it is necessary to program the output current distribution of the converter rationally. The equivalent circuit of n BUCK DC/DC converters is shown in Fig.3.

$$\eta = \frac{U_{\mathrm{o}}I_{\mathrm{o}}}{\sum\limits_{i=1}^{n} P_i} = \frac{U_{\mathrm{o}}I_{\mathrm{o}}}{\sum\limits_{i=1}^{n} \frac{U_{\mathrm{o}}I_{\mathrm{io}}}{\eta_i}} = \frac{I_{\mathrm{o}}}{\sum\limits_{i=1}^{n} \frac{I_{\mathrm{io}}}{\eta_i}} \tag{2}$$

$$I_{\mathrm{o}} = I_{1\mathrm{o}} + I_{2\mathrm{o}} + \ldots + I_{n\mathrm{o}} \tag{3}$$

where, P_{i} is the input power of module i, η_i is the efficiency of module i, I_{o} is total output current, U_{o} is output voltage, and η denotes total efficiency. From the formula (2)-(3), it can be found that the global optimal efficiency of the IPOP DC/DC converter system can be achieved by minimizing the denominator in Formula (2), which is the basic principle for efficiency optimization in this paper. In addition, output power limit of converter should also be considered according to the actual situation.

Based on the above analysis, the efficiency optimization problem of IPOP DC/DC system can be described as follows.

Objective Function:

$$\begin{cases} Min\{\sum\limits_{i=1}^{n} \frac{I_{\mathrm{io}}}{\eta_i}\} \\ \eta_i = ae^{bI_{\mathrm{io}}} + ce^{dI_{\mathrm{io}}} \end{cases} \tag{4}$$

Decision Variables:

$$\{I_{1\mathrm{o}}, I_{2\mathrm{o}}, \ldots, I_{n\mathrm{o}}\} \tag{5}$$

Linear Constraint:

$$\begin{cases} \sum\limits_{i=1}^{n} I_{\mathrm{io}} = I_{\mathrm{o}} \\ I_{\mathrm{iC}} < I_{\mathrm{io}} \leq I_{\mathrm{iR}} \end{cases} \tag{6}$$

where, I_{iC} is the critical current under continuous conduction mode (CCM) of module i, and I_{iR} is the rated current of module i.

B. PARAMETER IDENTIFICATION OF CONVERTER EFFICIENCY MODEL BASED ON LS ALGORITHM

LS algorithm is a mathematical optimization method, which minimizes the sum of squares errors to solve the optimal function or to carry out parameter identification. The LS algorithm for parameter identification can be described as formula (7), where $\boldsymbol{l} = [a, b, c, d]$ is parameter vector, $y(l, t_j)$ is the parameter function with weight, $\varphi(t_j)$ is the actual output value with weight, and t_j is the actual input value. The optimal parameter vector solution l can be obtained through formula (7). In formula (8), $f(x)$ replaced by $\sum_{i=1}^{n} I_{\mathrm{io}}/\eta_i$ can be further obtained.

$$\min_{l \in R^4} \sum_{j=1}^{M} \left(y(l, t_j) - \varphi(t_j)\right)^2 \tag{7}$$

$$\begin{cases} \min f(x) \\ s.t.\ \ h_i(x) = 0, \quad i \in E = \{1, \cdots, l\} \\ \quad\quad g_i(x) \geq 0, \quad i \in I = \{1, \cdots, m\} \end{cases} \tag{8}$$

C. CURRENT DISTRIBUTION COEFFICIENT OF CONVERTER UNIT BASED ON SQP ALGORITHM

SQP algorithm has good super-linear convergence and global convergence, and performs well in solving optimization problems with linear or nonlinear constraints. At present, SQP algorithm has become one of the most effective means to solve nonlinear optimization problems. The basic idea of SQP algorithm is to determine the descending direction by solving a quadratic programming sub-problem in each iteration step, and then obtain the corresponding step length according to the value function, and get the optimal solution by iterating repeatedly [24], [25].

In order to solve nonlinear optimization problem with constraints, SQP algorithm is used to work out control coefficient metric $\boldsymbol{x}^*$. As shown in Fig.4, the procedure of LS-SQP algorithm could be expressed as follows:

$$d_k = x - x_k \tag{9}$$

$$\begin{cases} \min \frac{1}{2} d^T H_K d + \nabla f(x_k)^T d \\ s.t.\ \ h_i(x_k) + \nabla h_i(x_k)^T = 0, \quad i \in E \\ g_i(x_k) + \nabla g_i(x_k)^T \geq 0, \quad i \in I \end{cases} \tag{10}$$

$$x_{k+1} = x_k + \alpha_k d_k \tag{11}$$

1) The linear constraint (6) obtained by LS algorithm are substituted into the formula (8).

2) Accuracy ε, maximum number of iterations M, initial starting point $\boldsymbol{x_0}$ and symmetric positive definite matrix $\boldsymbol{H_0} = \boldsymbol{E}$ are set. As shown in formula (10), the higher order term(>2) and constant term of objective function $f(x)$ are ignored by Taylor Formula at $\boldsymbol{x_k}$. The constraints of formula (10) are also linearized and the original nonlinear constrained optimization problem becomes QP problem.

3) If the error $\boldsymbol{d_K}$ of the solution of the sub-problem meets the accuracy, the output $\boldsymbol{x}^* = \boldsymbol{x_k}$ becomes the optimal solution. Otherwise, the appropriate line search procedure is selected to determine the step size α_k and the $\boldsymbol{x_k}$ is updated

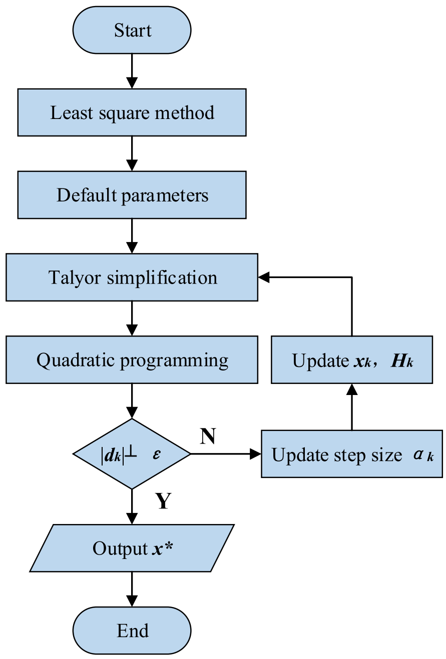

FIGURE 4. LS-SQP algorithm flow in the IPOP DC/DC system.

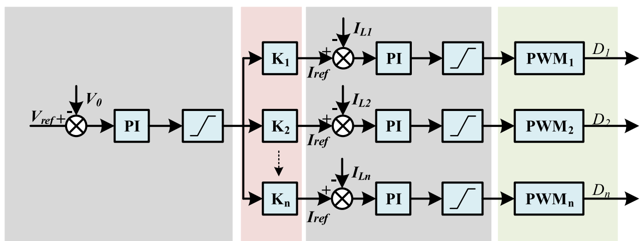

FIGURE 5. Proportional current distribution control strategy for IPOP DC/DC system.

by formula (11). After that, the formula of DFP or BFGS is used to modify $\boldsymbol{H}_{k+1}$, which is defined as the Hessian metric of $f(\boldsymbol{x}_{k+1})$. After repeated iteration, the cycle is completed when the accuracy ε meets the requirement or the maximum number of iteration is reached, the optimal solution $\boldsymbol{x}^* = [I_{1o}, I_{2o}, \ldots, I_{no}]$ is output, and the current distribution coefficient matrix $\boldsymbol{K} = \boldsymbol{x}^*/I_o$ is further obtained.

III. OPTIMAL EFFICIENCY CONTROL STRATEGY OF IPOP DC/DC SYSTEM

The IPOP DC/DC system adopts the proportional current distribution (PCD) control strategy, where each module shares the voltage outer loop with other modules but has independent current inner loop. The current distribution control is carried out by adjusting the output current distribution coefficient matrix $\boldsymbol{K}$.

A. PROPORTIONAL CURRENT DISTRIBUTION CONTROL STRATEGY FOR IPOP DC/DC SYSTEM

The IPOP DC/DC Buck converters are presented in Fig.5. Firstly, the voltage error signal is obtained by comparing the output voltage with the reference voltage. Afterwards, the voltage error signal is transferred to the PI, and the reference current of each converter is obtained according to

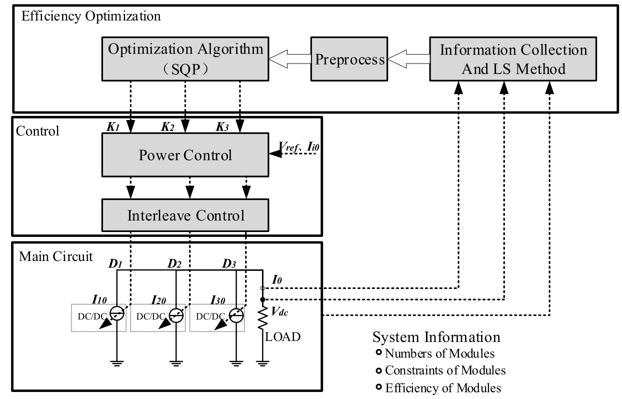

FIGURE 6. Structural block diagram of efficiency optimization for IPOP DC/DC system.

the current distribution coefficient matrix $\boldsymbol{K} = \boldsymbol{x}^*/I_o = [K_1, K_2, \ldots, K_n]$. Finally, the current error signal is obtained by comparing the current feedback with the reference current of each converter. The signal of duty ratio, which is obtained by PI and PWM, is transmitted to each module, so as to realize the power distribution of the system.

B. THE CONFIGURATION OF EFFICIENCY OPTIMIZATION OF SYSTEM

In this paper, the structure diagram of efficiency optimization of three-module IPOP DC/DC system is presented. As is shown in Fig.6, the system mainly consists of three parts: efficiency optimization algorithm, control strategy and main circuit. The main circuit can be equivalent to three current sources in parallel with the load. The control strategy receives the current distribution coefficient matrix $\boldsymbol{K}$ from the efficiency optimization program and controls the main circuit according to the PCD strategy. In addition, considering the larger output ripple of the IPOP DC/DC system, the interleaving (phase-shifted) control strategy can be adopted to suppress the ripple. Taking three-phase interleaving as an example, each phase is separated by 120°, which reduces the inductance volume and inhibits the ripple as well. The efficiency optimization algorithm program collects the load current, bus voltage and other system information of the main circuit. After preprocessing, LS-SQP algorithm is employed to solve the matrix K, which is then transferred to the control program to achieve the efficiency optimization.

C. DESIGN OF CONTROLLER PARAMETERS

It is assumed that DC/DC converters are ideal models without parasitic parameters. According to the averaging equivalent circuit method, the equivalent controlled source circuit of the IPOP DC/DC system is shown in Fig.7. By substituting the corresponding component parameters shown in Table.1 into (12), the corresponding open-loop transfer function can be derived as (14)-(15), as shown at the bottom of the next page.

1) DESIGN OF CURRENT LOOP CONTROLLER

The proposed current closed-loop system is shown in Fig.8, where $G_{id}(s)$ is the control to inductor current transfer

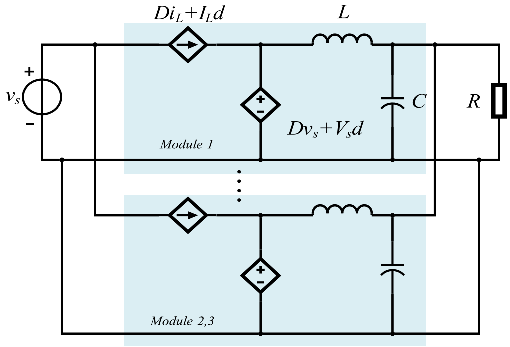

FIGURE 7. Small signal equivalent model of IPOP DC/DC system.

TABLE 1. Parameter setting of converters.

Category	Detail	Simulation/experiment	
Basic parameter	Converter	Buck (Module1,2,3)	
	Input/Output voltage	36/12V	
	Efficiency	$\eta_1>\eta_2>\eta_3$	—
Circuit parameter	Inductance L	330uH	5mH
	Capacitance C	470uF	470uF
	Switch frequency f	100kHz	10kHz
parasitic parameter	Inductance R_L	(0.12, 0.12,0.6)Ω	—
	Diode V_F	(0.5,0.8,0.8)V	—
	MOSFET R_{on}	(0.1,0.6,0.4)Ω	—

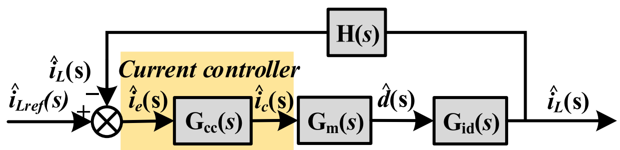

FIGURE 8. Current closed-loop scheme of IPOP DC/DC system.

function of DC/DC converter, $G_m(s)$ is the transfer function of pulse-width modulator, $H(s)$ denotes the feedback transfer function, and $G_{cc}(s)$ is the current controller transfer function. In the current closed-loop of DC/DC converter, the transfer function $G_m(s)$ =1, $H(s)$ =1 are utilized, and the transfer function $G_{cc}(s)$ of proportional integral (PI) controller is shown in (13). The PI controller parameters are K_{cp} =0.2, and K_{ci} =5. Therefore, the corresponding open-loop transfer function $G_{oc}(s)$ is obtained as (14).

As a result, the Bode diagrams of current open-loop transfer function can be obtained as shown in Fig.10(a). It can be seen that the amplitude margin h_c, and the phase margin γ_c are both greater than 0. The current closed-loop system can operate stably.

$$G_{id}(s) = \frac{G_{iv}(s)V_S}{LCs^2 + L/Rs + 1} = \frac{(Cs + 1/R)V_S}{LCs^2 + L/Rs + 1} \quad (12)$$

$$\begin{cases} G_{cc}(s) = K_{cp} + K_{ci}/s \\ G_{cv}(s) = K_{vp} + K_{vi}/s \end{cases} \quad (13)$$

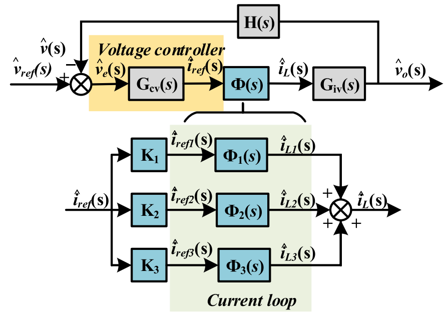

FIGURE 9. Voltage closed-loop scheme of IPOP DC/DC system.

2) DESIGN OF VOLTAGE LOOP CONTROLLER

The proposed voltage closed-loop system is shown in Fig.9, where $G_{iv}(s)$ is the output voltage to inductor current transfer function of DC/DC converter, $\Phi(s)$ is the transfer function of current closed-loop system, and $G_{cv}(s)$ is the voltage controller transfer function. The PI controller parameters are K_{vp} = 0.01, and K_{vi} = 200. The voltage open-loop transfer function $G_{ov}(s)$ is obtained as (15).

Likewise, as is shown in Fig.10(b), the voltage closed-loop can also be stable. Therefore, the controller parameter design of the system is completed.

IV. THE VERIFICATION OF SIMULATION AND EXPERIMENT

According to the PCD strategy proposed above, three DC/DC Buck converters are selected to form a three-module IPOP DC/DC system, and simulation is carried out to verify the effectiveness of efficiency optimization. The specific converter parameters are presented in Table 1. The software MATLAB/SIMULINK is used for simulation.

A. THE EFFICIENCY MODEL SOLUTION OF CONVERTER BASED ON LS ALGORITHM

The simulation of each Buck DC/DC converter module with variable load was carried out. The corresponding efficiency values of the three modules is presented in Table 2. $\boldsymbol{l} = [a, b, c, d]$ is obtained by LS algorithm, and then substituted into formula (1) to obtain the efficiency model of each Buck DC/DC converter module (16)-(18). Meanwhile, the maximum RMSE (Root Mean Squared Error) between the fitting and the actual result is 0.001063, which confirms the accuracy of proposed efficiency model.

The simulation result of each Buck DC/DC converter are shown in Fig.11. Taking module 3 as an example, three efficiency points which included (1.8A, 84.69%), (2.8A, 81.01%) and (3.8A, 77.205%) were selected as test points. Compared with the theoretical fitting results, RMSE is

$$G_{oi}(s) = G_{cc}(s)G_m(s)G_{id}(s) = \frac{1800(s + 25)(47s + 20000)}{47s^3 + 20000s^2 + 2.5 \times 10^7 s} \quad (14)$$

$$G_{ov}(s) = G_{cv}(s)\varphi(s)G_{iv}(s) = \frac{19881s^4 + 1.7814645 \times 10^7 s^3 + 4.3713405 \times 10^9 s^2 + 1.7046 \times 10^{11} s + 1.8 \times 10^{12}}{47000s^4 + 1.046 \times 10^8 s^3 + 6.3115 \times 10^{10} s^2 + 9 \times 10^{11} s} \quad (15)$$

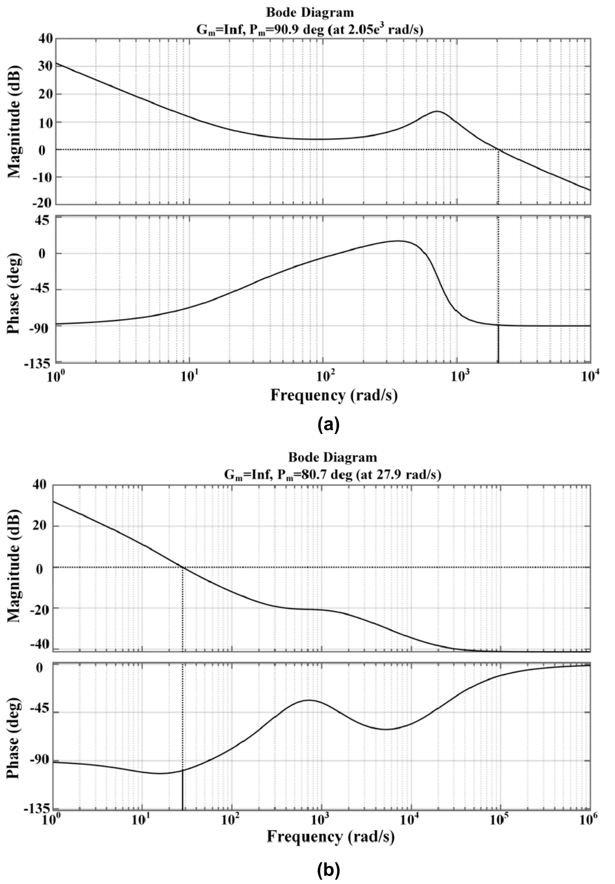

FIGURE 10. Bode diagrams of small-signal open-loop transfer functions. (a)current open-loop scheme. (b)voltage open-loop scheme.

TABLE 2. The simulating result of converter.

I_O/A	η_1/%	η_2/%	η_3/%
0.5	88.74	86.82	85.48
1	92.15	89.36	86.82
2	92.96	89.06	83.97
3	92.42	82.63	80.16
4	91.70	85.39	76.45
5	90.78	83.38	72.84
6	89.86	81.28	69.51

0.000744, which further verifies the effectiveness of LS algorithm for parameter identification with proposed efficiency model.

$$\eta_1 = 0.9517e^{-0.009577x} - 0.1646e^{-2.031x} \quad (16)$$
$$\eta_2 = 0.9396e^{-0.024x} - 0.1495e^{-1.824x} \quad (17)$$
$$\eta_3 = 0.9228e^{-0.04701x} - 0.1791e^{-2.694x} \quad (18)$$

B. THE SOLUTION OF CURRENT DISTRIBUTION BASED ON SQP ALGORITHM

The critical current I_{iC} is obtained according to formula (19) for the above three-module IPOP DC/DC system. As shown in formula (21), the initial point is $\boldsymbol{x_0} = [I_{1C}, I_{2C}, I_{3C}]$ and the rated current I_{iR} is 7A. Therefore, the constraint of optimization problem is determined. Objective function

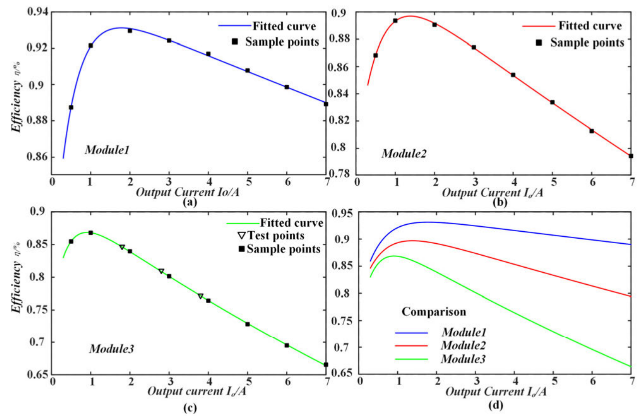

FIGURE 11. The simulating result of Buck DC/DC converters.

TABLE 3. The simulating result of IPOP DC/DC system.

Load current (I_o/A)	Current-sharing (η/%)	Current-distribution (η_k/%)	Current distribution metric (I_{1o},I_{2o},I_{3o}/A)
2	88.5	92.96	(2, 0, 0)
5	89.27	90.79	(3.509, 1.491, 0)
10	85.74	88.85	(6.415, 2.422, 1.163)
15	82.03	85.22	(7, 5.423, 2.577)
20	78.17	79.19	(7, 7, 6)

$f(x)$ is obtained by LS algorithm, and formulas (20)-(21) are obtained by the above constraints. The current distribution coefficient matrix $\boldsymbol{K}$, which is obtained by SQP algorithm, is substituted into the IPOP DC/DC control system for simulation. In addition, simulation was carried out based on the current-sharing control method as a comparison, and the result of simulation is shown in Table 3.

$$I_{iC} = \Delta I_i = \frac{V_{in} - V_o}{2L} DT_S \quad (19)$$

$$\begin{cases} \min \ f(x) = \sum_{i=1}^{3} I_{io}/\eta_i \\ s.t. \ A_{eq}x = b_{eq} \\ Ax \le b \end{cases} \quad (20)$$

$$\begin{cases} A_{eq} = \begin{bmatrix} 1 & 1 & 1 \end{bmatrix}, \ b_{eq} = I_0 \\ A = \begin{bmatrix} E_{3\times3} \\ -E_{3\times3} \end{bmatrix}, \ b = [I_{iR}, -I_{iC}]_{6\times1}^T \end{cases} \quad (21)$$

C. COMPARISONS WITH OTHER METHODS

Taking three-phase DC/DC converter systems as an example, the system efficiency of phase shedding mode, current-sharing mode and current-distribution mode are shown in the Fig.12. The conventional current-sharing mode is adopted, in which total power is evenly distributed. At any time, the converter with high equivalent impedance actually consumes more power. The phase-shedding (sequential turn-on) mode is adopted in [18]. The threshold current, which are obtained by advanced algorithm, can open two-phase current-sharing mode and three-phase current-sharing mode in turn.

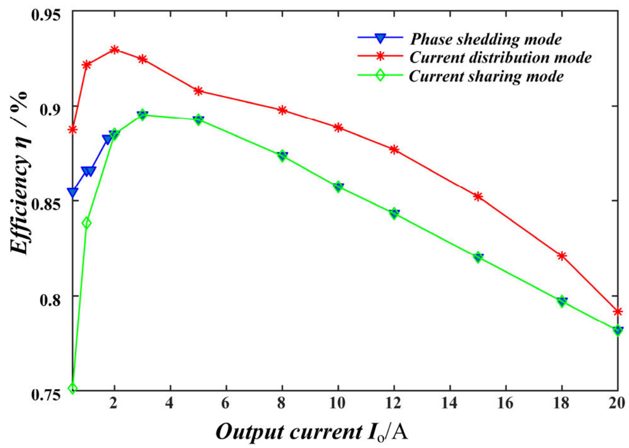

FIGURE 12. The efficiency comparisons with counterparts.

TABLE 4. The comparison with counterparts.

	Method in [7]	Method In [18]	Proposed method
Name	Current-sharing mode	Phase-shedding mode	Current distribution mode
Control strategy	Fixed	Fixed	Adjustable
Efficiency	low	medium	high
Sensor	4	4	4

Compared with threshold current, it can improve the global efficiency by switching phase. However, there is still room for efficiency optimization. With the combination of LS and SQP algorithm, adaptive power distribution and global efficiency optimization in the full load range can be realized.

As is shown in Table 4 and Fig.12, the proposed method is superior to current-sharing and phase-shedding mode in full load range. The above methods all employ three current sensors and a voltage sensor, and the conventional methods always guarantee the stability of IPOP DC/DC system with ignoring efficiency optimization. In addition, different from conventional the control strategy, the proposed PCD control strategy is adjustable between current-sharing mode and current distribution mode.

D. EXPERIMENTAL ANALYSIS

As shown in Fig.13, three Buck DC/DC converters are employed in IPOP DC/DC system as the prototype. In order to reflect the difference among modules, C2M0080120D, IRFP240 and STW20NK50Z are employed as MOSFETs in each module, respectively. The MAX471 chip is used in the current sampling circuit and the parallel resistance is used in the voltage sampling circuit. The controller is built based on MATLAB/SIMULINK, and then the controller is imported into STARSIM RCP (rapid control prototyping) software. The upper computer realizes the information interaction with the main circuit through the PXI interface box, where the whole closed-loop system is implemented.

Similar to the above simulation, the experiment for each Buck DC/DC converter module with variable load is carried out. The experimental results show that the maximum RMSE of the theoretical fitting curve of the converters is 0.001898. As shown in Fig.14, (1.8A, 90.271%), (2.8A, 87.972%) and (3.8A, 85.514%)are selected as test points. Compared with the theoretical fitting results, RMSE is 0.000744, which proves the accuracy of the LS algorithm based on the proposed efficiency model. In addition, the solution of efficiency model is substituted into SQP algorithm to achieve PCD. The experimental results are shown in Table 5 and Fig.14.

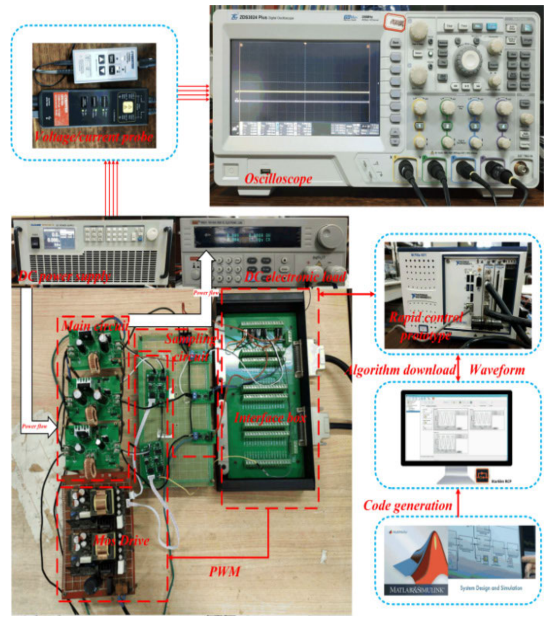

FIGURE 13. Experimental platform of IPOP DC/DC system.

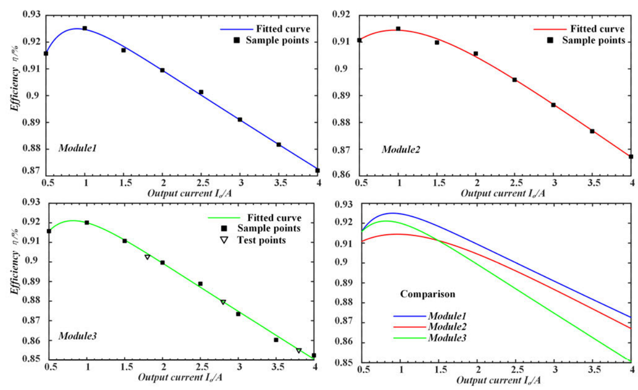

FIGURE 14. The experimental result of Buck DC/DC converters.

TABLE 5. The experimental result of IPOP DC/DC system.

Load current (I_o/A)	Current-sharing (η/%)	Current-distribution (η_k/%)	Current distribution metric (I_{1o}, I_{2o}, I_{3o}/A)
2	91.33	91.805	(0.828,0.5,0.672)
4	89.787	90.286	(1.401,1.452,1.174)
6	87.368	87.62	(2.156,2.143,1.702)
8	85.38	85.802	(2.944,2.8,2.256)
10	82.938	83.059	(3.723,3.454,2.823)

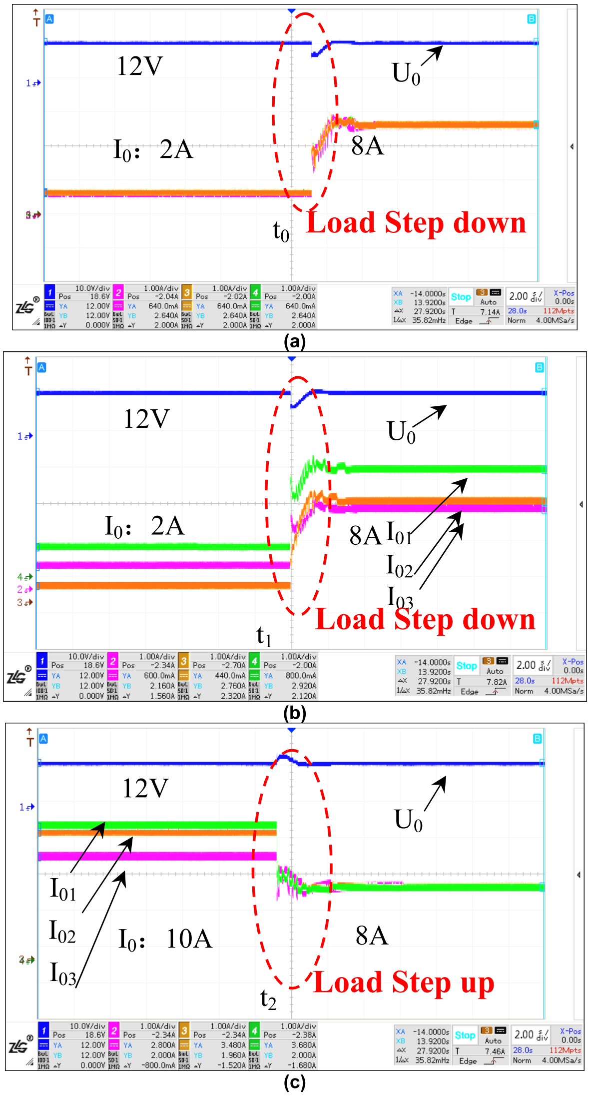

FIGURE 15. **The variable load experiment under the PCD strategy. (a) Current-sharing mode. (b) Current-distribution mode. (c) The switch between current-sharing and current-distribution working modes.**

In order to verify the effectiveness and superiority of the proposed control strategy, experiments with load step-change are carried out. In the IPOP DC/DC system, the waveforms of I_{1o}, I_{2o}, I_{3o} and U_o under different working modes are shown in Fig. 15(a), (b). As shown in Fig.15(a), at t_0, the load changes from 6Ω to 1.5Ω. It can be found that PCD control strategy has high accuracy, which can meet the requirements of the conventional current-sharing control strategy. As shown in Fig.15(b), when the load steps changing from 6Ω to 1.5Ω, the current distribution vector for efficiency optimization will change from $\boldsymbol{K} = [0.41, 0.25, 0.34]$ to $\boldsymbol{K} = [0.37, 0.35, 0.28]$. Furthermore, the PCD control strategy can realize the efficiency optimization of the system according to the change of $\boldsymbol{K}$. Seen from Fig.15(c), the current-distribution control is used in the parallel system before t_2. When the parallel system is operated at t_2, the operating mode changes to the current-sharing control. Meanwhile, the current distribution vector for efficiency optimization will change from $\boldsymbol{K} = [0.41, 0.25, 0.34]$ to $\boldsymbol{K} = [1/3, 1/3, 1/3]$. The flexible switch of working mode is realized, which is convenient to design the over current protection scheme.

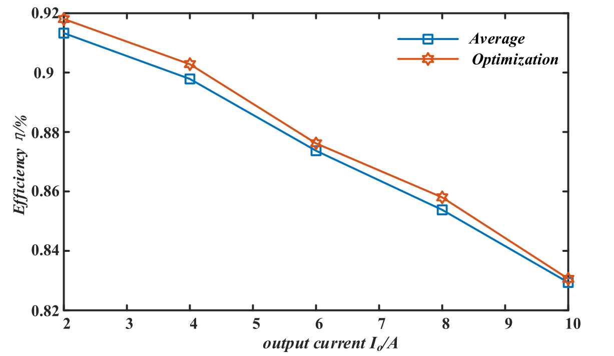

FIGURE 16. **Efficiency comparison of IPOP DC/DC system between optimized and average mode.**

The maximum RMSE of the theoretical model obtained by simulation and experiment is 0.001063 and 0.001898 respectively, so the effectiveness of LS algorithm for parameter identification with proposed efficiency model has been proved. Moreover, the efficiency of proposed control strategy is 4.46% higher than conventional strategy, which is presented in Table 3. In Fig.16 and Table 4, the experimental efficiency of PCD strategy is 0.48% higher than conventional current-sharing strategy, proving the effectiveness of proposed efficiency optimization algorithm as well.

V. CONCLUSION

In this paper, the efficiency modeling method of converter based on LS algorithm and the PCD control strategy based on SQP algorithm are proposed to optimize the overall efficiency of the system.

1) LS algorithm is adopted for parameter identification, in which the tedious loss analysis process is avoided. What is more, its maximum RMSE is 0.001898 that effectively reflects the true efficiency characteristic of converter during the full load range;

2) The SQP algorithm is used to obtain the optimal power distribution solution for each paralleled converter, where the limitation of converter power is taken into account. Therefore, there is no need to add/reduce converters for secondary optimization;

3) On the basis of the proposed algorithm, the PCD control strategy is adopted to realize the flexible switch between current-sharing mode and current-distribution mode. The global optimal efficiency is increased by 4.46% and 0.48% in simulation and experiment, respectively.

In this paper, confirmatory experiment is carried out, and the next work is to develop a higher power module.

REFERENCES

[1] F. V. Cerna, M. Pourakbari-Kasmaei, M. Lehtonen, and J. Contreras, "Efficient automation of an HEV heterogeneous fleet using a two-stage methodology," *IEEE Trans. Veh. Technol.*, vol. 68, no. 10, pp. 9494–9506, Oct. 2019.

[2] B. Zhang, H. Lim, S. Xu, and W. Su, "Distance-oriented hierarchical control and ecological driving strategy for HEVs," *IET Elect. Syst. Transp.*, vol. 9, no. 1, pp. 44–52, Mar. 2019.

[3] H. Li, F. Ren, C. Liu, Z. Guo, J. Lü, B. Zhang, and T. Q. Zheng, "An extended stability analysis method for paralleled DC–DC converters system with considering the periodic disturbance based on Floquet theory," *IEEE Access*, vol. 8, pp. 9023–9036, 2020.

[4] H. Wang, M. Han, R. Han, J. M. Guerrero, and J. C. Vasquez, "A decentralized current-sharing controller endows fast transient response to parallel DC–DC converters," *IEEE Trans. Power Electron.*, vol. 33, no. 5, pp. 4362–4372, May 2018.

[5] G. Chen and X. Cai, "Adaptive control strategy for improving the efficiency and reliability of parallel wind power converters by optimizing power allocation," *IEEE Access*, vol. 6, pp. 6138–6148, 2018.

[6] M. Ashourloo, V. R. Namburi, G. V. Pique, J. Pigott, H. J. Bergveld, A. E. Sherif, and O. Trescases, "Decentralized quasi-fixed-frequency control of multiphase interleaved hybrid dickson converters for fault-tolerant automotive applications," *IEEE Trans. Power Electron.*, vol. 35, no. 7, pp. 7653–7663, Jul. 2020.

[7] Y. Xia, M. Yu, Y. Peng, P. Lin, D. Shi, and W. Wei, "Circulating currents suppression for IPOP nonisolated DC/DC converters based on modified topologies," *IEEE Trans. Power Electron.*, vol. 34, no. 2, pp. 1901–1913, Feb. 2019.

[8] Y. Xia, M. Yu, Y. Peng, and W. Wei, "Modeling and analysis of circulating currents among input-parallel output-parallel nonisolated converters," *IEEE Trans. Power Electron.*, vol. 33, no. 10, pp. 8412–8426, Oct. 2018.

[9] Y. Wang, K. Wang, C. Li, Z. Zheng, and Y. Li, "System-level efficiency evaluation of isolated DC/DC converters in power electronics transformers for medium-voltage DC systems," *IEEE Access*, vol. 7, pp. 48445–48458, 2019.

[10] Y. Wang, C. Wang, L. Xu, J. Meng, and Y. Hei, "Adjustable inertial response from the converter with adaptive droop control in DC grids," *IEEE Trans. Smart Grid*, vol. 10, no. 3, pp. 3198–3209, May 2019.

[11] L. He, J. Chen, X. Xu, B. Cheng, J. Sun, D. Guo, and J. Nai, "Soft-switching voltage-demultiplier-cell-based high step-down DC–DC converter," *IEEE Trans. Power Electron.*, vol. 34, no. 10, pp. 9828–9843, Oct. 2019.

[12] A. Asghari, "Ultra-high step-down ZVS synchronous buck converter with low switch voltage stress," *IET Power Electron.*, vol. 13, no. 10, pp. 2039–2048, Aug. 2020.

[13] C.-O. Yeon, J.-W. Kim, M.-H. Park, I.-O. Lee, and G.-W. Moon, "Improving the light-load regulation capability of LLC series resonant converter using impedance analysis," *IEEE Trans. Power Electron.*, vol. 32, no. 9, pp. 7056–7067, Sep. 2017.

[14] L. He, J. Chen, B. Cheng, and H. Zhou, "Duty cycle loss compensation method based on magnetic flux cancelation in high-current high-frequency synchronous rectifier of LCLC converter," *IEEE Trans. Power Electron.*, vol. 36, no. 1, pp. 103–113, Jan. 2021.

[15] R. Suryadevara, T. Li, K. Modepalli, and L. Parsa, "IPOP-connected FB-ZCS DC–DC converter modules for renewable energy integration with medium-voltage DC grids," *IEEE Trans. Ind. Appl.*, vol. 55, no. 5, pp. 5128–5140, Sep./Oct. 2019.

[16] A. Vazquez, A. Rodriguez, D. G. Lamar, and M. M. Hernando, "Advanced control techniques to improve the efficiency of IPOP modular QSW-ZVS converters," *IEEE Trans. Power Electron.*, vol. 33, no. 1, pp. 73–86, Jan. 2018.

[17] S. A. Arshadi, M. Ordonez, W. Eberle, M. Craciun, and C. Botting, "Three-phase LLC battery charger: Wide regulation and improved light-load operation," *IEEE Trans. Power Electron.*, vol. 36, no. 2, pp. 1519–1531, Feb. 2021.

[18] A. Stupar, T. McRae, N. Vukadinović, A. Prodić, and J. A. Taylor, "Multi-objective optimization of multi-level DC–DC converters using geometric programming," *IEEE Trans. Power Electron.*, vol. 34, no. 12, pp. 11912–11939, Dec. 2019.

[19] S. Wang, J. Liu, Z. Liu, T. Wu, and B. Liu, "Efficiency-based optimization of steady-state operating points for parallel source converters in stand-alone power system," in *Proc. IEEE 8th Int. Power Electron. Motion Control Conf. (IPEMC-ECCE Asia)*, Hefei, China, May 2016, pp. 163–170.

[20] W. Yuan, Y. Wang, D. Liu, and F. Deng, "Adaptive droop control strategy of autonomous microgrid for efficiency improvement," in *Proc. IEEE 10th Int. Symp. Power Electron. Distrib. Gener. Syst. (PEDG)*, Xi'an, China, Jun. 2019, pp. 972–977.

[21] X. Lyu, N. Ren, and D. Cao, "Optimal configuration of high-efficiency segmented linear LED driver with genetic algorithm," *IEEE J. Emerg. Sel. Topics Power Electron.*, vol. 7, no. 1, pp. 209–215, Mar. 2019.

[22] H. Li, D. Yang, W. Su, J. Lu, and X. Yu, "An overall distribution particle swarm optimization MPPT algorithm for photovoltaic system under partial shading," *IEEE Trans. Ind. Electron.*, vol. 66, no. 1, pp. 265–275, Jan. 2019.

[23] Y. Wang, Z. Su, Q. Xu, T. Yang, and N. Zhang, "A novel charging scheme for electric vehicles with smart communities in vehicular networks," *IEEE Trans. Veh. Technol.*, vol. 68, no. 9, pp. 8487–8501, Sep. 2019.

[24] C. Zhang, H. Chen, K. Shi, Z. Liang, W. Mo, and D. Hua, "A multi-time reactive power optimization under interval uncertainty of renewable power generation by an interval sequential quadratic programming method," *IEEE Trans. Sustain. Energy*, vol. 10, no. 3, pp. 1086–1097, Jul. 2019.

[25] Y. Chen, M. Bruschetta, D. Cuccato, and A. Beghi, "An adaptive partial sensitivity updating scheme for fast nonlinear model predictive control," *IEEE Trans. Autom. Control*, vol. 64, no. 7, pp. 2712–2726, Jul. 2019.

FENGWANG LU was born in Jiangsu, China, in 1995. He received the B.Sc. degree in mechanical engineering from the Yancheng Institute of Technology, Yancheng, in 2018. He is currently pursuing the M.S. degree with the Department of Instrumental and Electrical Engineering, Xiamen University.

His research interests include dc-dc converters, optimization algorithm, and new energy system efficiency.

LIANGZONG HE was born in Hunan, China, in 1984. He received the B.Sc. degree from Jilin University, Changchun, China, in 2006, and the Ph.D. degree from the Huazhong University of Science and Technology, Wuhan, China, in 2012. From November 2009 to August 2011, he was a joint Ph.D. education student with Michigan State University, East Lansing, MI, USA. In September 2012, he joined Xiamen University, Xiamen, China, as an Assistant Professor, and has been a Professor, since August 2019. His research interests include dc-dc converters, switched-capacitor converters, Z-source converters, wireless power transmission, and microgrid.

QINGYANG TAN received the B.E. degree from Sichuan University, Chengdu, China, in 2019. She is currently pursuing the M.S. degree with the Department of Power Electronics, Xiamen University, Xiamen, China. Her research interests include dc-dc converters.

HONGYAN ZHOU was born in Hebei, China, in 1998. He received the B.Sc. degree in electrical engineering from Xiamen University, Xiamen, in 2019, where he is currently pursuing the M.S. degree with the Department of Instrumental and Electrical Engineering.

His research interests include high power density dc-dc converters and new energy system stability.